

pubs.acs.org/ac Article

Through-Space Multinuclear Magnetic Resonance Signal Enhancement Induced by Parahydrogen and Radiofrequency Amplification by Stimulated Emission of Radiation

Oleg G. Salnikov,* Ivan A. Trofimov, Andrey N. Pravdivtsev, Kolja Them, Jan-Bernd Hövener, Eduard Y. Chekmenev, and Igor V. Koptyug



Cite This: Anal. Chem. 2022, 94, 15010-15017



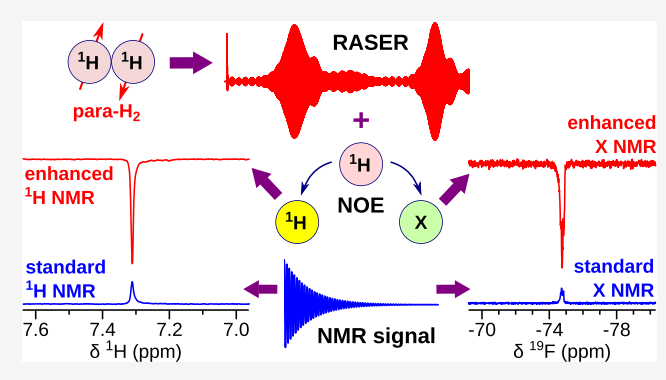
ACCESS I

III Metrics & More

Article Recommendations

Supporting Information

ABSTRACT: Hyperpolarized (*i.e.*, polarized far beyond the thermal equilibrium) nuclear spins can result in the radiofrequency amplification by stimulated emission of radiation (RASER) effect. Here, we show the utility of RASER to amplify nuclear magnetic resonance (NMR) signals of solute and solvent molecules in the liquid state. Specifically, parahydrogen-induced RASER was used to spontaneously enhance nuclear spin polarization of protons and heteronuclei (here $^{19}{\rm F}$ and $^{31}{\rm P})$ in a wide range of molecules. The magnitude of the effect correlates with the T_1 relaxation time of the target nuclear spins. A series of control experiments validate the through-space dipolar mechanism of the RASER-assisted polarization transfer between the parahydrogen-polarized compound and to-be-hyperpolarized nuclei of the target molecule. Frequency-



selective saturation of the RASER-active resonances was used to control the RASER and the amplitude of spontaneous polarization transfer. Spin dynamics simulations support our experimental RASER studies. The enhanced NMR sensitivity may benefit various NMR applications such as mixture analysis, metabolomics, and structure determination.

■ INTRODUCTION

Inherently low sensitivity is seen as a significant limitation of NMR spectroscopy and imaging. The most efficient way to improve NMR sensitivity is to create nuclear spin hyperpolarization, i.e., highly nonequilibrium population of the nuclear spin states.^{1,2} At the moment, several hyperpolarization techniques are available, including dissolution dynamic nuclear polarization (d-DNP),³⁻⁵ spin-exchange optical pumping (SEOP),^{6–8} parahydrogen-induced polarization (PHIP),⁵ and signal amplification by reversible exchange (SABRE). 14,15 d-DNP and SEOP are currently used for human biomedical applications with astounding results.8,16-18 However, d-DNP and SEOP require sophisticated and expensive equipment limiting their widespread use and suffer from the long time needed for production of a hyperpolarized (HP) sample and the low duty cycles. In contrast, PHIP and SABRE are the faster and more affordable alternatives. Both methods employ parahydrogen $(p-H_2)$, the singlet spin isomer of dihydrogen, as a spin order source. The PHIP technique is based on the pairwise addition of p-H₂ to an unsaturated precursor at high or low magnetic fields (PASADENA^{9,19} and ALTADENA²⁰ experiments, respectively). In SABRE, both parahydrogen and substrate molecules undergo reversible exchange on a metal complex; within the complex, nuclear spin polarization is transferred from the p-H2-derived hydrides to a coordinated

substrate via spin—spin couplings. ^{14,21} PHIP and SABRE allow one to obtain more than 50% nuclear spin polarization within seconds ^{22,23} and with high duty cycles. ²⁴ However, these techniques are substrate-specific. PHIP polarizes only compounds for which the corresponding unsaturated precursors exist. For SABRE, the substrate should transiently coordinate to the metal complex. ^{21,25} The recently proposed SABRE-Relay ^{26–28} and PHIP-X²⁹ approaches expand the scope of polarizable compounds to those with exchangeable protons, although the currently attainable target polarization levels are significantly lower than those for compounds directly polarized by PHIP or SABRE.

The radiofrequency amplification by stimulated emission of radiation (RASER) effect was previously shown for optically pumped ³He and ¹²⁹Xe³⁰ and in DNP experiments. ^{31–34} Recently, RASER was also demonstrated in SABRE and PHIP experiments. ^{35–40} The detailed description of the RASER

Received: July 7, 2022
Accepted: October 7, 2022
Published: October 20, 2022





theory can be found elsewhere.³⁹ In brief, RASER is a result of a nonlinear interaction of negatively hyperpolarized nuclear spins with the resonant circuit of the NMR probe. The RASER emission starts if population inversion is high enough and continues as long as high population inversion is maintained. The Fourier transform (FT) of the RASER NMR signal can result in dramatically narrowed NMR lines with the full width at half-maximum (FWHM) of several mHz.^{34,35} The RASER emission can be triggered or starts spontaneously so that the MR signal can be acquired without the application of a radiofrequency (RF) pulse allowing for background-free detection of HP compounds.⁴¹ Also, the small difference in the initial population inversion density inducing RASER can be employed as a source of contrast for magnetic resonance imaging (MRI).⁴²

Another phenomenon related to hyperpolarization techniques is the spin polarization-induced nuclear Overhauser effect (SPINOE)—spontaneous transfer of polarization from HP species to other molecules in solution via dipole-dipole interactions.⁴³ SPINOE was previously demonstrated with optically pumped $^{129}\mathrm{Xe}^{43-45}$ and with $[1,4^{-13}\mathrm{C}_2]$ fumarate hyperpolarized by d-DNP. 46 Recently, optical polarization of pentacene-doped naphthalene crystals was also employed as an efficient SPINOE hyperpolarization source. 47 SPINOE was not reported for PHIP and SABRE effects alone. However, recently, Korchak et al. demonstrated that if PASADENA hyperpolarization is high enough to initiate the RASER activity, ¹H resonances of the solvent or the solute (shown on the example of N-acetylated amino acid) are enhanced via dipolar interactions.⁴⁸ This effect was called PRINOE (parahydrogen and RASER-induced NOE).⁴⁸ Herein, we investigate the efficiency of PRINOE hyperpolarization of a broad range of substrates. We show that the PRINOE approach can be employed for hyperpolarization of other nuclei beyond protons (e.g., ¹⁹F and ¹³¹P). Moreover, we demonstrate that both ALTADENA and PASADENA RASERs can provide PRINOE effects, and we propose the use of saturation of the RASER-active resonances with the train of soft RF pulses for increasing the PRINOE efficiency.

■ EXPERIMENTAL SECTION

Here, the typical procedure of the PHIP RASER experiments is described. In several experiments, we made some modifications to this typical procedure—these specific experimental details can be found in the Supporting Information (SI). Commercially available vinyl acetate (Sigma-Aldrich, ≥99%), bis-(norbornadiene)rhodium(I) tetrafluoroborate ([Rh(NBD)₂]-BF₄, NBD = norbornadiene, Strem 45-0230, \geq 96%), 1,4bis(diphenylphosphino)butane (dppb, Sigma-Aldrich, 98%), methanol-d₄ (CIL, 99.8% D), and ultrapure hydrogen (>99.999%) were used as received. Hydrogen gas was enriched with p-H₂ to a 98-99% content using a parahydrogen generator based on a closed-cycle helium cryostat (CryoPribor, CFA-200-H2CELL) and a cryocompressor (Sumitomo, Zephyr HC-4A). Hydrated iron oxide FeO(OH) (Sigma-Aldrich, 371254) was used in a cell as a spin conversion catalyst. For the sample preparation, vinyl acetate (VA) was dissolved in CD₃OD, and the obtained solution was added to the mixture of [Rh(NBD)₂]BF₄ and dppb. The amounts of reactants were calculated to get concentrations of VA and Rh complex of 0.8 M and 10 mM, respectively; dppb was taken in a \sim 2% excess with respect to Rh. The solution was left for \sim 30 min with periodic mixing to ensure formation of the

[Rh(NBD)(dppb)]BF₄ ([Rh]) complex. The resultant solution (0.6 mL) was placed in a standard 5 mm Wilmad NMR tube tightly connected with a 1/4 in. outer diameter PTFE tube. Optionally, the required amount of the target compound (e.g., benzene) was added to provide a 0.8 M concentration. The scheme of the experimental setup is presented in Figure 1b. The gas lines were purged with p-H₂ for \sim 1 min. The

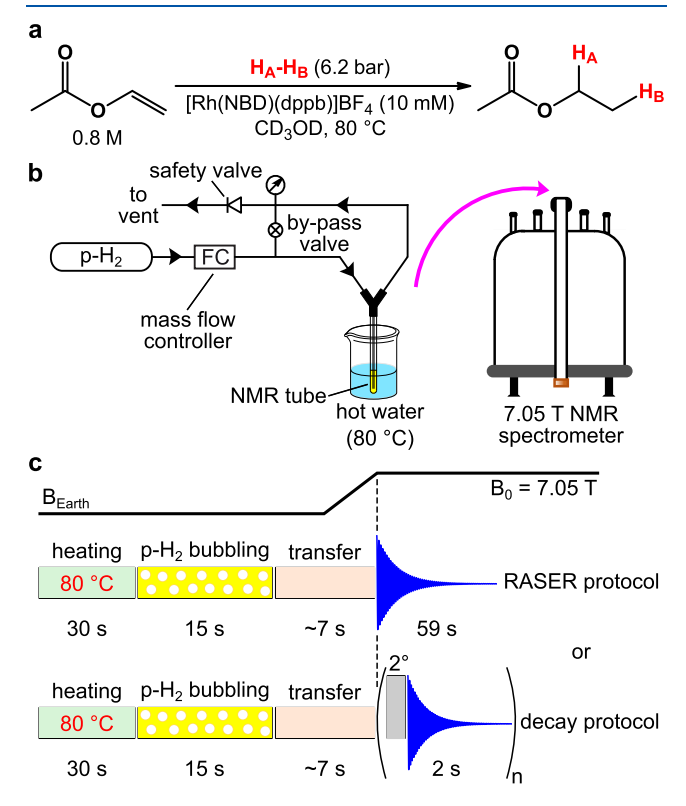


Figure 1. (a) Reaction scheme of vinyl acetate hydrogenation with p-H $_2$ to yield HP ethyl acetate. (b) Scheme of the experimental setup used for RASER and PRINOE experiments. (c) Event sequence in RASER and decay protocol experiments. In the RASER protocol, the 1 H NMR signal was acquired for 59 s without the application of an RF excitation pulse. In the decay protocol, a series of 1 H NMR spectra were acquired after the application of 2° RF excitation pulses with a 2 s repetition time.

sample was connected to the gas lines and pressurized to 6.2 bar (regulated by a 75 psig safety valve) while the bypass valve (see Figure 1b) was opened. The sample was heated to 80 °C in a beaker with hot water for 30 s. Then, p-H₂ bubbling was initiated by closing the bypass valve; the gas was bubbled at a 100 standard cubic centimeters per minute (sccm) gas flow rate for 15 s. The gas flow rate was regulated using a mass flow controller (Brooks Instrument, model 5850E). Next, the sample was rapidly taken out from the beaker, dried with a paper towel, and placed into the NMR probe of a 7.05 T Bruker AV 300 NMR spectrometer. The sample transfer time was ~7 s. A 5 mm PH DUL 300S1 C-H-D-05 CIDNP NMR probe with a Q factor of ca. 550 was utilized. The temperature of the NMR probe was set at 297 K. NMR signal acquisition was started ~1 s before the sample was placed into the NMR probe. In the RASER protocol experiments, the NMR signal was acquired without the application of an RF excitation pulse (acquisition time = 59.14 s). These experiments were performed without the addition of the target compound. In the decay protocol experiments, a series of NMR spectra were

acquired with the application of 2° RF excitation pulses with a 2 s repetition time.

RESULTS AND DISCUSSION

ALTADENA RASER Effects. To initiate the RASER, pairwise addition of p- H_2 to vinyl acetate over the homogeneous $[Rh(NBD)(dppb)]BF_4$ catalyst to form HP ethyl acetate (EA) was performed (Figure 1a). To achieve high-amplitude initial magnetization required to initiate the RASER activity, we used a high initial VA concentration of 0.8 M. Hydrogenation of VA was performed via bubbling of p- H_2 at the Earth's magnetic field (ALTADENA conditions 20) using the experimental setup presented in Figure 1b. The RASER effect was probed either using the RASER protocol or using the decay protocol (see Figure 1c and the Experimental Section). The observed RASER signals and the corresponding FT spectra were generally similar to the previously published results 37 and are presented and described in details in the SI (see Figures S1 and S2).

Observation of PRINOE Effects. Normally, after ALTADENA hyperpolarization of EA using the [Rh] catalyst, PHIP effects are observed for the EA ethyl moiety, norbornene, and norbornane. However, in the RASER experiments described above, essentially all other protons present in the solution were also hyperpolarized: the acetyl CH₃ group of EA (which has a negligible J coupling to the protons of the ethyl moiety and thus is normally not hyperpolarized in ALTADENA experiments 19, all protons of unreacted VA, and the residual protons of the methanol-d₄ solvent (Figure 2). These results suggested a hyperpolarization transfer to molecules not involved in the hydrogenation reaction, which was investigated further.

Indeed, we found that other molecules can be hyperpolarized in the same way, when added to the solution, even if they are not expected to chemically interact with the catalyst, p- H_2 and EA. For convenience, we call such added chemicals as target compounds throughout this article. We chose benzene as a model target compound because its ¹H chemical shift is far away from HP EA signals, and it has 6 equivalent protons giving an intensive NMR signal. The concentration of target compounds was 0.8 M—equal to that of VA in the starting solutions. Notably, all protons, which showed these abnormal polarization effects, had emissive (*i.e.*, negative) NMR signals. This spontaneous hyperpolarization of chemically inactive compounds in solution in the presence of PHIP RASER is a result of the parahydrogen and RASER-induced NOE (PRINOE) effect recently introduced by Korchak *et al.* ⁴⁸

The kinetics of target compound signal enhancement (SE) was probed via the decay protocol (acquisition of a series of NMR spectra after application of 2° RF pulses with a 2 s repetition time). SE was estimated as the ratio of integrals of the corresponding lines measured for the spectra of hyperpolarized and thermally polarized solutions, respectively. Note that we include the sign of the NMR signal integral in SE calculations, resulting in negative SE for emissive signals. The SPINOE kinetic curve for benzene showed the clear maximum (for convenience, here and later on SPINOE curves are discussed in terms of absolute SE values) at t = 48 s after the sample was placed into the NMR probe of a 7.05 T NMR spectrometer, $SE_{max} = -3.4$ (Figure 3). This SE was obtained at 60% conversion of VA to EA with a 12.5% initial ¹H polarization of the EA HA proton (Figure 3). The biexponential fit of the benzene SE kinetic curve according

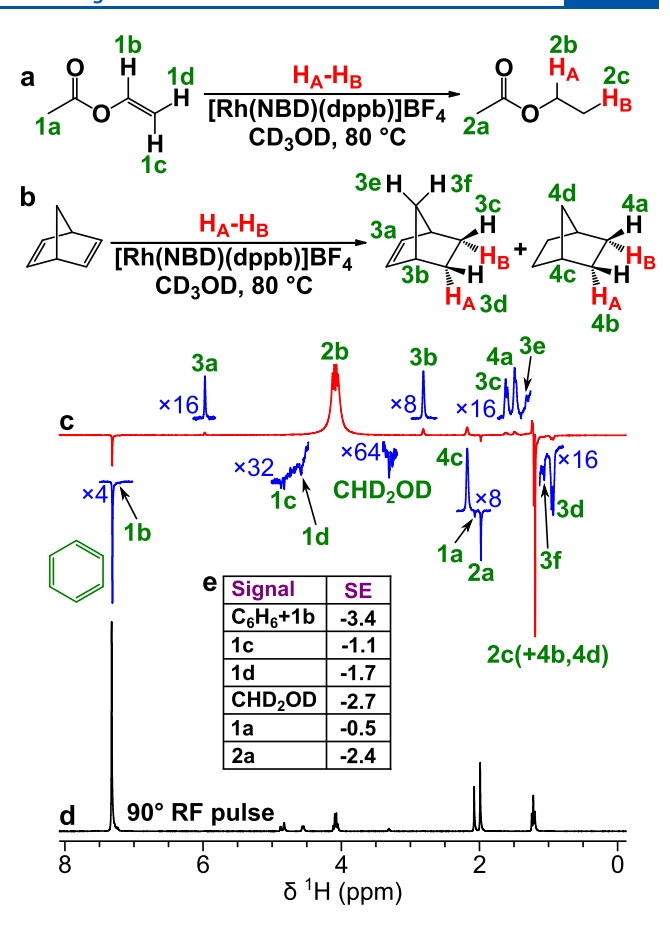


Figure 2. (a) Reaction scheme of VA hydrogenation with $p\text{-H}_2$ to yield HP EA. (b) Reaction scheme of NBD hydrogenation with $p\text{-H}_2$ to yield HP norbornene and norbornane. (c) ^1H NMR spectrum acquired in ALTADENA hyperpolarization of EA using the decay protocol with a 2° RF excitation pulse 48 s after the sample is placed in the NMR probe with benzene added as a target (the blue insets show magnified signals of HP compounds). (d) Thermal reference spectrum of the same solution acquired using a 90° RF pulse after relaxation of hyperpolarization. The NMR spectra were recorded at 7.05 T. (e) Signal enhancement factors (SE) observed for the SPINOE-hyperpolarized protons in spectrum (c). SE is the ratio of integrals of the corresponding lines with and without hyperpolarization.

to the SPINOE formula⁴⁸ yields characteristic rise and decay time constants $t_1 = 31.1 \pm 0.8$ s and $t_2 = 65 \pm 1$ s (Figure 3).

PRINOE Mechanism. Previously, PRINOE was observed in PASADENA conditions⁴⁸ resulting in initial multiplet antiphase polarization of EA, which is then converted to the net in-phase positive magnetization by the action of RASER. The resultant highly nonequilibrium total nuclear spin polarization of EA induces hyperpolarization of other compounds present in the solution via dipolar interactions (*i.e.*, SPINOE effect). According to SPINOE theory, ^{43,48} the sign of the SPINOE effect is the opposite to the sign of the polarization source. Thus, positive hyperpolarization of EA induces negative SPINOE signals of the target compounds. ⁴⁸

Here, in ALTADENA experiments, EA initially possesses net polarization of individual spins, but the signals of its H_A and H_B protons have different signs resulting in close to zero total net magnetization of the molecule. In this case, the spontaneous NOE polarization transfers from H_A and H_B protons are expected to compensate each other leading to a

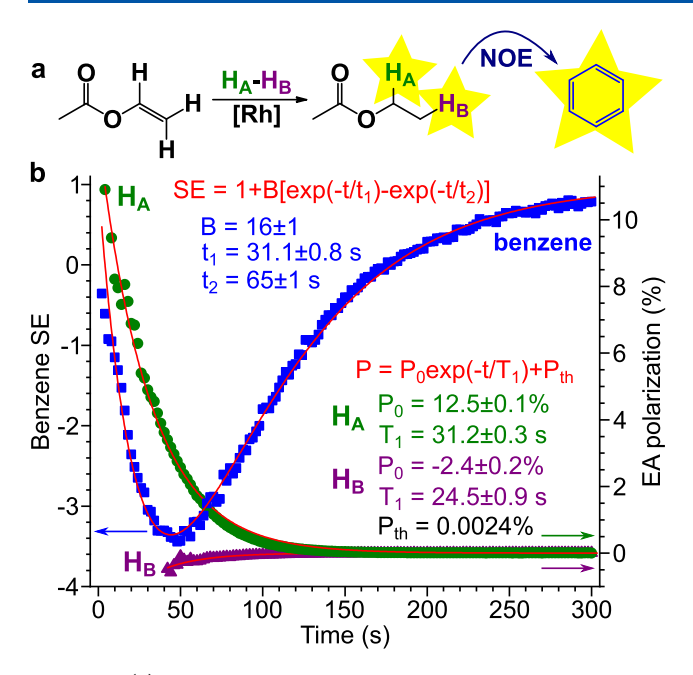


Figure 3. (a) Reaction scheme of VA hydrogenation with $p\text{-H}_2$ to yield HP EA with a subsequent NOE polarization transfer to benzene as a target molecule. (b) Kinetics of SPINOE ¹H NMR signal enhancement of benzene (blue squares, left *Y*-axis) and simultaneous decay of EA ¹H hyperpolarization (green circles, H_A proton, and purple triangles, H_B proton, right *Y*-axis). The initial data points for polarization of the H_B proton were excluded due to the strong RASER effects. The data were measured using the decay protocol (signal acquisition after a 2° RF excitation pulse, repetition time of 2 s) at 7.05 T. The ¹H NMR spectrum at t=48 s is presented in Figure 2c.

zero total SPINOE. Because of this, the ALTADENA approach was believed to be hardly suitable for SPINOE hyperpolarization of other compounds present in the solution. However, our results demonstrate that this is not the case.

In ALTADENA experiments, the emerging RASER activity significantly suppresses the signal of the negatively polarized spin ($H_{\rm B}$ proton of EA in our case) resulting in positive total nuclear spin polarization, as confirmed experimentally (see Figure 3b) and by the spin dynamics simulations (see the Supporting Information). This high positive net magnetization induces negative polarization on the target (and other) molecules via dipolar interactions.

To verify the PRINOE mechanism for ALTADENA, we performed two additional experiments. First, the HP sample was kept at 7.05 T but outside of the RF coil for 20 s, allowing for relaxation of EA polarization below the RASER threshold. When this sample was finally moved into the RF coil region and its ¹H NMR spectrum was acquired, no polarization on the benzene target was observed (details in the SI, Figure S3). Second, a 5 mm NMR tube with the solution of the [Rh] catalyst and VA in CD₃OD was placed inside a 10 mm tube with DMSO- d_6 . The benzene target was added either to the inner or to the outer tube. In the decay protocol ALTADENA experiments with these two sample compositions, hyperpolarization of benzene was observed only when it was in the solution with HP EA (details in the SI, Figure S4). Together, these experiments prove that both the RASER effect and the short-distance intermolecular interactions are necessary for hyperpolarization of the target compounds.

Manipulating PRINOE with Frequency-Selective RF Pulses. In the subsequent experiments, we investigated the

effect of saturation of the EA ¹H NMR resonances with a train of soft 90° RF pulses on the PRINOE polarization of the target molecule. When the resonance of the EA CH2 group (HA, positively polarized in ALTADENA) was saturated followed by the application of a hard 90° RF pulse and FID acquisition, SE = -0.9 was obtained for the benzene target (Figure S7). The saturation of the EA CH₃ signal (H_B, negatively polarized in ALTADENA) yielded SE = -4.9, while in a control experiment, when no soft pulses were applied, SE = -3.9was obtained. These results proved that hyperpolarization was transferred from EA to the target compound via SPINOE since the magnitude of NOE polarization transfer should be proportional to the difference in polarization of H_A and H_B spins of EA. Moreover, application of frequency-selective pulses manifests itself as a tool to control PRINOE hyperpolarization.

Solvent and Temperature Effects. The efficiency of short-distance intermolecular polarization transfer via NOE depends on the molecular mobility, which can be controlled by the solvent viscosity and temperature. First, we changed the solvent from CD₃OD to acetone- d_6 . In this case, the ALTADENA RASER effect was observed, but the NMR signal of the benzene target was positive throughout the time window of the decay NMR spectra acquisition (Figure S8). However, the kinetics of benzene signal evolution was qualitatively similar to the SPINOE curve presented in Figure 3b with the minimum at t = 20 s. Therefore, it can be concluded that the PRINOE effect is operating in the case of the acetone- d_6 solvent, but it is not strong enough to shift the target signal to negative values. Weaker PRINOE in acetone-d₆ is primarily caused by the lower conversion of VA to EA (32% vs ~61%) and the lower EA polarization levels (4% vs \sim 12%, H_A proton), resulting in an ~6 times lower initial magnetization amenable to SPINOE transfer to the target molecules. Another factor is the lower viscosity of acetone- d_6 leading to higher mobility of molecules and a shorter average time window for the intermolecular polarization transfer by NOE (although here, the effect of viscosity is inferior to the effect of the initial polarization of EA).

The temperature effect on PRINOE efficiency was investigated by varying the temperature inside the NMR probe in the range of 268-308 K while keeping the reaction temperature at 353 K to maintain the HP EA yield and polarization. Unfortunately, the temperature range available for this study was rather limited because at higher temperatures the hydrogenation reaction can continue to a significant extent while the sample resides in the NMR probe. This would definitely affect the PRINOE dynamics and magnitude. Although the exact temperature of the sample throughout this experiment is not known, the measurements by a Bruker variable temperature (VT) unit show that the temperature of the NMR probe rises only by ~ 1 K after the preheated sample is placed inside the detecting coil. This indicates that the sample cooling inside the probe is rather efficient and that the better part of the PRINOE dynamics proceeds at the constant temperature set by the VT unit. No significant difference in benzene SE was detected in the probed temperature range (Figure S9d), likely because both the relaxation rate and the rate of SPINOE polarization transfer (or the NOE crossrelaxation rate) decrease with temperature.5

PHIP Substrate and Target Molecule Effects. When 2-hydroxyethyl acrylate (HEA) was used as a PHIP precursor to produce HP 2-hydroxyethyl propionate (HEP), RASER effects

were observed similar to the case of EA (Figure S10). PRINOE enhancement was detected for the benzene target albeit at a low intensity with $SE_{max} = -0.2$ (Figure S11). Again, the lower efficiency of PRINOE is correlated with the lower polarization levels of HP HEP compared to HP EA (3.35% vs ~12%).

Next, we explored the scope of target molecules amenable to PRINOE hyperpolarization. Amines (benzyl amine and ethanolamine) deactivate the catalyst likely via irreversible coordination to the Rh center, completely preventing EA production. Carboxylic acids (malonic and citric acids) also deactivate the catalyst but not completely—in this case, HP EA was formed but with the significantly lower polarization and conversion levels (Table S1). The obtained molar polarization P_{EA}^{M} values of 1.7 and 1.4 mM, respectively, are not high enough for the RASER initiation. As a result, the target protons are not hyperpolarized. Most of the other target compounds tested (methanol, benzyl alcohol, hydroguinone, N,N-dimethyl formamide, benzene, furan, dichloromethane, and chloroform) did not show any effects on the catalyst performance, yielding ca. 60-70% conversion of VA to EA and a $P_{\rm EA}$ of ca. 10-12% corresponding to ca. 45-60 mM $P_{\rm EA}^{\rm M}$ (Table S1). Interestingly, the dimethyl sulfoxide (DMSO) target boosts the catalyst activity resulting in full consumption of VA after 15 s of p-H₂ bubbling but at the expense of EA polarization. As a result, a P_{EA}^{M} of 52 mM is obtained in the case of DMSO, which is similar to the case of other target compounds (Table S1). The increased VA hydrogenation efficiency in the presence of DMSO can be attributed to coordination of DMSO to the [Rh] catalyst, promoting its activity.

The maximum PRINOE signal enhancement observed for the target molecules clearly correlates with their T_1 relaxation times (Table 1 and Figure S12). The most efficiently

Table 1. Maximum PRINOE Signal Enhancements (SE_{max}) and T_1 Relaxation Times for Various Target Compounds

target compound	SE_{max}	$\begin{array}{c} {\rm SE}_{\rm max}/P^{M}_{\rm EA}, \\ {\rm M}^{-1} \end{array}$	T_1 , s ^a
N,N -dimethyl formamide b	-1.0 ± 0.1	-16 ± 5	4.59 ± 0.06
hydroquinone	-1.3 ± 0.4	-22 ± 5	6.93 ± 0.06
dimethyl sulfoxide	-1.2 ± 0.2	-23 ± 4	7.61 ± 0.05
dichloromethane	-2.1 ± 1.2	-42 ± 20	16.2 ± 0.3
methanol	-1.7 ± 0.8	-26 ± 7	17.1 ± 0.2
benzyl alcohol ^c	-1.4 ± 1.0	-31 ± 13	22.1 ± 0.2
benzene	-3.1 ± 0.8	-54 ± 9	56 ± 2
furan	-4.5 ± 1.2^d	-83 ± 11^{d}	92 ± 6^{d}
	-4.4 ± 1.0^{e}	-82 ± 6^{e}	87 ± 1 ^e
chloroform	-3.7 ± 0.7	-65 ± 9	96 ± 6

 aT_1 measured at 297 K for the samples after hydrogenation in CD₃OD. b Data for the formyl proton. c Data for the combined signal of the aromatic protons. d Data for the protons in positions 2 and 5. e Data for the protons in positions 3 and 4. f Additional data for these target compounds are presented in Table S1 in the SI. Examples of PRINOE kinetic curves are presented in Figure S13.

hyperpolarized compound was furan with SE_{max} = -4.5 ± 1.2 for the protons in positions 2 and 5 ($T_1 = 92 \pm 6$ s) and SE_{max} = -4.4 ± 1.0 for the protons in positions 3 and 4 ($T_1 = 87 \pm 1$ s). Also, the strong enhancement of SE_{max} = -3.7 ± 0.7 was obtained for CHCl₃ ($T_1 = 96 \pm 6$ s). The obtained values are in line with the results of Korchak *et al.* who showed an SE of up to -4.4 for CHCl₃.

To show the viability of PRINOE for NMR signal enhancement of more biologically relevant compounds, we investigated ethyl pyruvate as a target. Hyperpolarized ethyl pyruvate is a prospective contrast agent for metabolic MRI, especially for brain imaging. S1-53 PRINOE polarization of ethyl pyruvate resulted in SE_{max} = -2.9 for the protons of the acetyl group of its keto form (Figure S14). Detection of PRINOE for other protons of ethyl pyruvate (the acetyl group of the hemiacetal form and the ethyl group) was complicated due to their overlap with the strongly enhanced $^1\mathrm{H}$ NMR signals of HP EA.

Heteronuclear PRINOE. Finally, we demonstrate that PRINOE can be employed for hyperpolarization of other nuclei beyond ¹H. The ¹⁹F nuclei of fluorinated compounds CF₃CO₂Et, (CF₃)₂CHOH (HFIP), CF₃CH(OH)₂, and CF₃CH(OH)(OEt) were polarized in the presence of the ¹H ALTADENA RASER inside the probe of a 1.4 T benchtop NMR spectrometer (Figure 4a and Figure S14). Ethyl trifluoroacetate demonstrated $SE_{max} = -1.25$, while the other three compounds provided the same averaged $SE_{max} = -6.8$ (Table S2). Similar to ¹H PRINOE, the observed ¹⁹F signal enhancements show correlation with the corresponding T_1 relaxation times—for CF_3CO_2Et , T_1 was shorter than those for the other target compounds (Table S2). The PRINOE hyperpolarization of ³¹P nuclei of hexamethylphosphoramide d_{18} (HMPA- d_{18}) (Figure 4b) yielded SE_{max} = -0.7 ± 0.1 (Table S3). We expect that 13C or 15N nuclei can be hyperpolarized using PRINOE in a similar way. Experimental proof of this assumption is not trivial because one needs to use an isotopically labeled target compound to get a detectable PRINOE signal. Moreover, this compound should meet other requirements such as (i) high solubility in methanol (this excludes simple inorganic salts), (ii) no effect on the catalyst activity (this excludes popular SABRE substrates 21,54 and carboxylic acids), and (iii) no C=C or C≡C bonds (this excludes PHIP-SAH precursors⁵⁵). Therefore, the investigation of ¹³C and ¹⁵N PRINOE requires the synthesis of carefully designed isotopically labeled compounds and is the subject of a future study.

CONCLUSIONS

In this work, we demonstrate that spontaneous SPINOE hyperpolarization of protons and heteronuclei in solution can be achieved in ALTADENA experiments with a high-field RASER effect. Spin dynamics simulations and experiments proved that radiation damping converts the ALTADENA spin order to positive net magnetization of the two spins, which induces negative magnetization onto the target spins via dipolar interactions. We show that frequency-selective saturation of the RASER-active spin increases the efficiency of PRINOE signal enhancement of the target compound. Investigation of the broad range of target molecules revealed that the attained signal enhancements correlate with the T_1 relaxation times of the corresponding spins. The largest ¹H PRINOE enhancements were obtained for furan, chloroform, and benzene. Moreover, the PRINOE approach can be employed for NMR signal enhancement of prospective metabolic MRI contrast agents such as ethyl pyruvate. Finally, we show that PRINOE is applicable not only for hyperpolarization of protons but also for heteronuclei, as demonstrated on the example of ¹⁹F and ³¹P. The increased sensitivity is especially promising for analytical applications of NMR. We envision that PRINOE NMR signal enhancement

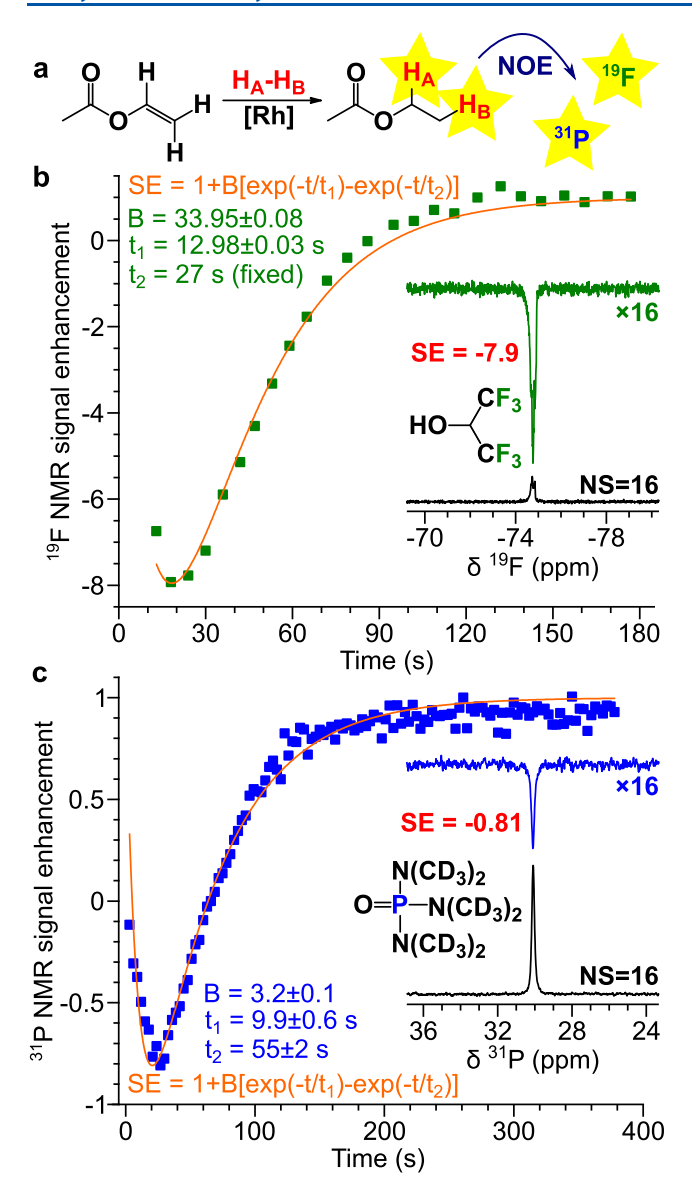


Figure 4. (a) Reaction scheme of VA hydrogenation with p-H₂ to yield HP EA with a subsequent NOE polarization transfer to 19F or ³¹P nuclei. (b) Kinetics of PRINOE ¹⁹F NMR signal enhancement of HFIP. The data were measured using the decay protocol (signal acquisition every 6-8 s with the application of a 6.5° RF excitation pulse) at 1.4 T. The inset shows the ¹⁹F NMR spectrum of PRINOEhyperpolarized HFIP acquired 18 s after the sample is placed in the NMR probe (top blue trace, multiplied by a factor of 16) and the thermal reference 19F NMR spectrum of the same solution acquired with 16 signal accumulations (bottom black trace). (c) Kinetics of PRINOE 31 P NMR signal enhancement of HMPA- d_{18} . The data were measured using the decay protocol (signal acquisition every 3 s with the application of a 6° RF excitation pulse) at 7.05 T. The inset shows the ³¹P NMR spectrum of PRINOE-hyperpolarized HMPA-d₁₈ acquired 27 s after the sample is placed in the NMR probe (top blue trace, multiplied by a factor of 16) and the thermal reference ³¹P NMR spectrum of the same solution acquired with 16 signal accumulations (bottom black trace).

may be exploited in the same way as SABRE hyperpolarization, which has shown its utility for analysis of natural extracts ⁵⁶ and biofluids. ^{57,58} The detailed study of the concentration dependence of PRINOE effects is warranted to explore the prospects of their analytical chemistry applications. Although current implementation of PRINOE does not provide similarly

impressive NMR signal enhancements of the solute molecules as a recently reported alternative approach based on triplet-DNP of pentacene-doped naphthalene, ⁴⁷ the PHIP RASER approach benefits from significantly faster polarization buildup (seconds vs 2–3 h) and, unlike triplet-DNP, does not require highly specialized polarization equipment and high purity of polarization source material. Future optimization of the PHIP precursor nature and experimental conditions will hopefully increase the NMR signal gain provided by the PRINOE approach in order to make it more efficient for new NMR applications.

ASSOCIATED CONTENT

Supporting Information

The Supporting Information is available free of charge at https://pubs.acs.org/doi/10.1021/acs.analchem.2c02929.

Modifications to the typical experimental procedure in the specific experiments; calculations of NMR signal enhancement and polarization levels; additional results, NMR spectra, plots, and tables: RASER effects at 7.05 and 1.4 T, control experiments proving the requirement of RASER and short-distance intermolecular interactions for PRINOE, PASADENA RASER effects, experiments with the frequency-selective RF pulses, solvent and temperature variation effects, experiments with 2-hydroxyethyl propionate as a polarization source, correlation of PRINOE signal enhancement with the target T_1 , PRINOE kinetics for various target compounds, and 19 F and 31 P PRINOE experiments; RASER simulations (PDF)

AUTHOR INFORMATION

Corresponding Author

Oleg G. Salnikov — International Tomography Center SB RAS, 630090 Novosibirsk, Russia; Boreskov Institute of Catalysis SB RAS, 630090 Novosibirsk, Russia; orcid.org/0000-0003-2266-7335; Email: salnikov@tomo.nsc.ru

Authors

Ivan A. Trofimov – International Tomography Center SB RAS, 630090 Novosibirsk, Russia; Novosibirsk State University, 630090 Novosibirsk, Russia

Andrey N. Pravdivtsev – Section Biomedical Imaging, Molecular Imaging North Competence Center (MOIN CC), Department of Radiology and Neuroradiology, University Medical Center Schleswig-Holstein and Kiel University, 24118 Kiel, Germany; orcid.org/0000-0002-8763-617X

Kolja Them — Section Biomedical Imaging, Molecular Imaging North Competence Center (MOIN CC), Department of Radiology and Neuroradiology, University Medical Center Schleswig-Holstein and Kiel University, 24118 Kiel, Germany; orcid.org/0000-0002-5512-0910

Jan-Bernd Hövener — Section Biomedical Imaging, Molecular Imaging North Competence Center (MOIN CC),
Department of Radiology and Neuroradiology, University
Medical Center Schleswig-Holstein and Kiel University,
24118 Kiel, Germany; ⊚ orcid.org/0000-0001-7255-7252

Eduard Y. Chekmenev – Department of Chemistry, Integrative Biosciences (Ibio), Karmanos Cancer Institute (KCI), Wayne State University, Detroit, Michigan 48202,

United States; Russian Academy of Sciences, 119991 Moscow, Russia; orcid.org/0000-0002-8745-8801 Igor V. Koptyug — International Tomography Center SB RAS, 630090 Novosibirsk, Russia; orcid.org/0000-0003-3480-7649

Complete contact information is available at: https://pubs.acs.org/10.1021/acs.analchem.2c02929

Author Contributions

O.G.S. and I.A.T. performed hyperpolarization experiments, data processing, and original draft preparation. A.N.P. performed RASER simulations. O.G.S supervised the project. I.V.K. and O.G.S. acquired funding. All coauthors interpreted the data, discussed the results, and proofread the manuscript. The project originated from the experiment suggested by E.Y.C. All authors have given approval to the final version of the manuscript.

Notes

The authors declare the following competing financial interest(s): E.Y.C. has a stake of ownership in XEUS Technologies LTD.

Although Korchak *et al.*⁴⁸ have a priority of the first peer-reviewed demonstration of PRINOE effects, we discovered these effects independently and presented the preliminary results at the PERM conference⁵⁹ a month earlier than when the work of Korchak *et al.* was published.

ACKNOWLEDGMENTS

O.G.S. thanks the Council on Grants of the President of the Russian Federation (grant MK-2826.2022.1.3) and the Russian Foundation for Basic Research (grant 19-33-60045) for the support of RASER studies. I.A.T. thanks the Russian Science Foundation (grant 21-73-10105) for the support of PRINOE hyperpolarization experiments. The Novosibirsk team thanks the Russian Ministry of Science and Higher Education for the access to NMR equipment. A.N.P., J.B.H., and K.T. acknowledge funding from the German Federal Ministry of Education and Research (BMBF) within the framework of the e:Med research and funding concept (01ZX1915C), DFG (PR 1868/ 3-1, HO-4602/2-2, HO-4602/3, GRK2154-2019, EXC2167, FOR5042, SFB1479, and TRR287). MOIN CC was founded by a grant from the European Regional Development Fund (ERDF) and the Zukunftsprogramm Wirtschaft of Schleswig-Holstein (project no. 122-09-053). E.Y.C. thanks the following for funding support: NSF under Grant CHE-1904780, the National Cancer Institute under 1R21CA220137, DOD CDMRP under W81XWH-20-10576, NIBIB under R01EB029829, and NHLBI R21 HL154032.

REFERENCES

- (1) Kovtunov, K. V.; Pokochueva, E. V.; Salnikov, O. G.; Cousin, S. F.; Kurzbach, D.; Vuichoud, B.; Jannin, S.; Chekmenev, E. Y.; Goodson, B. M.; Barskiy, D. A.; Koptyug, I. V. *Chem. Asian J.* **2018**, 13, 1857–1871.
- (2) Kondo, Y.; Nonaka, H.; Takakusagi, Y.; Sando, S. Angew. Chem., Int. Ed. 2021, 60, 14779–14799.
- (3) Pinon, A. C.; Capozzi, A.; Ardenkjær-Larsen, J. H. Magn. Reson. Mater. Phys., Biol. Med. 2021, 34, 5-23.
- (4) Ceillier, M.; Cala, O.; El Daraï, T.; Cousin, S. F.; Stern, Q.; Guibert, S.; Elliott, S. J.; Bornet, A.; Vuichoud, B.; Milani, J.; Pages, C.; Eshchenko, D.; Kempf, J. G.; Jose, C.; Lambert, S. A.; Jannin, S. J. Magn. Reson. Open 2021, 8–9, 100017.

- (5) Ardenkjær-Larsen, J. H.; Fridlund, B.; Gram, A.; Hansson, G.; Hansson, L.; Lerche, M. H.; Servin, R.; Thaning, M.; Golman, K. *Proc. Natl. Acad. Sci. U. S. A.* **2003**, *100*, 10158–10163.
- (6) Goodson, B. M. J. Magn. Reson. 2002, 155, 157-216.
- (7) Khan, A. S.; Harvey, R. L.; Birchall, J. R.; Irwin, R. K.; Nikolaou, P.; Schrank, G.; Emami, K.; Dummer, A.; Barlow, M. J.; Goodson, B. M.; Chekmenev, E. Y. *Angew. Chem., Int. Ed.* **2021**, *60*, 22126–22147.
- (8) Marshall, H.; Stewart, N. J.; Chan, H.-F.; Rao, M.; Norquay, G.; Wild, J. M. Prog. Nucl. Magn. Reson. Spectrosc. 2021, 122, 42–62.
- (9) Bowers, C. R.; Weitekamp, D. P. J. Am. Chem. Soc. 1987, 109, 5541-5542.
- (10) Hövener, J.-B.; Pravdivtsev, A. N.; Kidd, B.; Bowers, C. R.; Glöggler, S.; Kovtunov, K. V.; Plaumann, M.; Katz-Brull, R.; Buckenmaier, K.; Jerschow, A.; Reineri, F.; Theis, T.; Shchepin, R. V.; Wagner, S.; Bhattacharya, P.; Zacharias, N. M.; Chekmenev, E. Y. Angew. Chem., Int. Ed. 2018, 57, 11140–11162.
- (11) Reineri, F.; Cavallari, E.; Carrera, C.; Aime, S. Magn. Reson. Mater. Phys., Biol. Med. 2021, 34, 25-47.
- (12) Buljubasich, L.; Franzoni, M. B.; Münnemann, K. Top. Curr. Chem. 2013, 338, 33–74.
- (13) Buntkowsky, G.; Theiss, F.; Lins, J.; Miloslavina, Y. A.; Wienands, L.; Kiryutin, A.; Yurkovskaya, A. RSC Adv. 2022, 12, 12477–12506.
- (14) Adams, R. W.; Aguilar, J. A.; Atkinson, K. D.; Cowley, M. J.; Elliott, P. I. P.; Duckett, S. B.; Green, G. G. R.; Khazal, I. G.; López-Serrano, J.; Williamson, D. C. Science 2009, 323, 1708–1711.
- (15) Rayner, P. J.; Duckett, S. B. Angew. Chem., Int. Ed. 2018, 57, 6742-6753.
- (16) Nelson, S. J.; Kurhanewicz, J.; Vigneron, D. B.; Larson, P. E. Z.; Harzstark, A. L.; Ferrone, M.; van Criekinge, M.; Chang, J. W.; Bok, R.; Park, I.; Reed, G.; Carvajal, L.; Small, E. J.; Munster, P.; Weinberg, V. K.; Ardenkjaer-Larsen, J. H.; Chen, A. P.; Hurd, R. E.; Odegardstuen, L.-I.; Robb, F. J.; Tropp, J.; Murray, J. A. Sci. Transl. Med. 2013, 5, 198ra108.
- (17) Kurhanewicz, J.; Vigneron, D. B.; Ardenkjaer-Larsen, J. H.; Bankson, J. A.; Brindle, K.; Cunningham, C. H.; Gallagher, F. A.; Keshari, K. R.; Kjaer, A.; Laustsen, C.; Mankoff, D. A.; Merritt, M. E.; Nelson, S. J.; Pauly, J. M.; Lee, P.; Ronen, S.; Tyler, D. J.; Rajan, S. S.; Spielman, D. M.; Wald, L.; Zhang, X.; Malloy, C. R.; Rizi, R. *Neoplasia* **2019**, *21*, 1–16.
- (18) Stewart, N. J.; Smith, L. J.; Chan, H.-F.; Eaden, J. A.; Rajaram, S.; Swift, A. J.; Weatherley, N. D.; Biancardi, A.; Collier, G. J.; Hughes, D.; Klafkowski, G.; Johns, C. S.; West, N.; Ugonna, K.; Bianchi, S. M.; Lawson, R.; Sabroe, I.; Marshall, H.; Wild, J. M. Br. J. Radiol. 2022, 95, 20210207.
- (19) Bowers, C. R.; Weitekamp, D. P. Phys. Rev. Lett. 1986, 57, 2645–2648.
- (20) Pravica, M. G.; Weitekamp, D. P. Chem. Phys. Lett. 1988, 145, 255-258.
- (21) Barskiy, D. A.; Knecht, S.; Yurkovskaya, A. V.; Ivanov, K. L. Prog. Nucl. Magn. Reson. Spectrosc. 2019, 114–115, 33–70.
- (22) Korchak, S.; Mamone, S.; Glöggler, S. ChemistryOpen 2018, 7, 672-676.
- (23) Fekete, M.; Ahwal, F.; Duckett, S. B. J. Phys. Chem. B 2020, 124, 4573-4580.
- (24) Schmidt, A. B.; Zimmermann, M.; Berner, S.; de Maissin, H.; Müller, C. A.; Ivantaev, V.; Hennig, J.; von Elverfeldt, D.; Hövener, J.-B. *Commun. Chem.* **2022**, *5*, 21.
- (25) Pravdivtsev, A. N.; Hövener, J.-B. Chem. Eur. J. 2019, 25, 7659-7668.
- (26) Iali, W.; Rayner, P. J.; Duckett, S. B. Sci. Adv. 2018, 4, No. eaao6250.
- (27) Rayner, P. J.; Tickner, B. J.; Iali, W.; Fekete, M.; Robinson, A. D.; Duckett, S. B. *Chem. Sci.* **2019**, *10*, 7709–7717.
- (28) Richardson, P. M.; Iali, W.; Roy, S. S.; Rayner, P. J.; Halse, M. E.; Duckett, S. B. *Chem. Sci.* **2019**, 10607–10619.
- (29) Them, K.; Ellermann, F.; Pravdivtsev, A. N.; Salnikov, O. G.; Skovpin, I. V.; Koptyug, I. V.; Herges, R.; Hövener, J. B. *J. Am. Chem. Soc.* **2021**, *143*, 13694–13700.

- (30) Chupp, T. E.; Hoare, R. J.; Walsworth, R. L.; Wu, B. *Phys. Rev. Lett.* **1994**, 72, 2363–2366.
- (31) Bösiger, P.; Brun, E.; Meier, D. Phys. Rev. Lett. 1977, 38, 602-605.
- (32) Chen, H.-Y.; Lee, Y.; Bowen, S.; Hilty, C. J. Magn. Reson. 2011, 208, 204–209.
- (33) Weber, E. M. M.; Kurzbach, D.; Abergel, D. Phys. Chem. Chem. Phys. **2019**, 21, 21278–21286.
- (34) Hope, M. A.; Björgvinsdóttir, S.; Grey, C. P.; Emsley, L. J. Phys. Chem. Lett. **2021**, 12, 345–349.
- (35) Suefke, M.; Lehmkuhl, S.; Liebisch, A.; Blümich, B.; Appelt, S. *Nat. Phys.* **2017**, *13*, 568–572.
- (36) Pravdivtsev, A. N.; Sönnichsen, F. D.; Hövener, J. B. ChemPhysChem **2020**, 21, 667–672.
- (37) Joalland, B.; Ariyasingha, N. M.; Lehmkuhl, S.; Theis, T.; Appelt, S.; Chekmenev, E. Y. *Angew. Chem., Int. Ed.* **2020**, *59*, 8654–8660.
- (38) Appelt, S.; Lehmkuhl, S.; Fleischer, S.; Joalland, B.; Ariyasingha, N. M.; Chekmenev, E. Y.; Theis, T. J. Magn. Reson. 2021, 322, No. 106815.
- (39) Appelt, S.; Kentner, A.; Lehmkuhl, S.; Blümich, B. Prog. Nucl. Magn. Reson. Spectrosc. 2019, 114–115, 1–32.
- (40) TomHon, P. M.; Han, S.; Lehmkuhl, S.; Appelt, S.; Chekmenev, E. Y.; Abolhasani, M.; Theis, T. *ChemPhysChem* **2021**, 22, 2526–2534.
- (41) Joalland, B.; Theis, T.; Appelt, S.; Chekmenev, E. Y. Angew. Chem., Int. Ed. 2021, 60, 26298–26302.
- (42) Lehmkuhl, S.; Fleischer, S.; Lohmann, L.; Rosen, M. S.; Chekmenev, E. Y.; Adams, A.; Theis, T.; Appelt, S. Sci. Adv. 2022, 8, No. eabp8483.
- (43) Ñavon, G.; Song, Y. Q.; Rõõm, T.; Appelt, S.; Taylor, R. E.; Pines, A. Science 1996, 271, 1848–1851.
- (44) Song, Y.-Q.; Goodson, B. M.; Taylor, R. E.; Laws, D. D.; Navon, G.; Pines, A. Angew. Chem., Int. Ed. Engl. 1997, 36, 2368–2370.
- (45) Cherubini, A.; Payne, G. S.; Leach, M. O.; Bifone, A. Chem. Phys. Lett. 2003, 371, 640-644.
- (46) Marco-Rius, I.; Bohndiek, S. E.; Kettunen, M. I.; Larkin, T. J.; Basharat, M.; Seeley, C.; Brindle, K. M. Contrast Media Mol. Imaging 2014, 9, 182–186.
- (47) Eichhorn, T. R.; Parker, A. J.; Josten, F.; Müller, C.; Scheuer, J.; Steiner, J. M.; Gierse, M.; Handwerker, J.; Keim, M.; Lucas, S.; Qureshi, M. U.; Marshall, A.; Salhov, A.; Quan, Y.; Binder, J.; Jahnke, K. D.; Neumann, P.; Knecht, S.; Blanchard, J. W.; Plenio, M. B.; Jelezko, F.; Emsley, L.; Vassiliou, C. C.; Hautle, P.; Schwartz, I. *J. Am. Chem. Soc.* 2022, 144, 2511–2519.
- (48) Korchak, S.; Kaltschnee, L.; Dervisoglu, R.; Andreas, L.; Griesinger, C.; Glöggler, S. Angew. Chem., Int. Ed. 2021, 60, 20984—20990
- (49) Salnikov, O. G.; Chukanov, N. V.; Shchepin, R. V.; Manzanera Esteve, I. V.; Kovtunov, K. V.; Koptyug, I. V.; Chekmenev, E. Y. J. Phys. Chem. C 2019, 123, 12827–12840.
- (50) Kowalewski, J.; Mäler, L. Nuclear Spin Relaxation in Liquids, 2nd ed.; CRC Press: 2006.
- (51) Hurd, R. E.; Yen, Y.-F.; Mayer, D.; Chen, A.; Wilson, D.; Kohler, S.; Bok, R.; Vigneron, D.; Kurhanewicz, J.; Tropp, J.; Spielman, D.; Pfefferbaum, A. *Magn. Reson. Med.* **2010**, *63*, 1137–1143.
- (52) Carrera, C.; Cavallari, E.; Digilio, G.; Bondar, O.; Aime, S.; Reineri, F. *ChemPhysChem* **2021**, *22*, 1042–1048.
- (53) Brahms, A.; Pravdivtsev, A. N.; Stamp, T.; Ellermann, F.; Sönnichsen, F. D.; Hövener, J.-B.; Herges, R. *Chem. Eur. J.* **2022**, 28, No. e202201210.
- (54) Chukanov, N. V.; Shchepin, R. V.; Joshi, S. M.; Kabir, M. S. H.; Salnikov, O. G.; Svyatova, A.; Koptyug, I. V.; Gelovani, J. G.; Chekmenev, E. Y. *Chem. Eur. J.* **2021**, *27*, 9727–9736.
- (55) Chukanov, N. V.; Salnikov, O. G.; Shchepin, R. V.; Kovtunov, K. V.; Koptyug, I. V.; Chekmenev, E. Y. ACS Omega **2018**, *3*, 6673–6682.

- (56) Hermkens, N. K. J.; Eshuis, N.; Van Weerdenburg, B. J. A.; Feiters, M. C.; Rutjes, F. P. J. T.; Wijmenga, S. S.; Tessari, M. *Anal. Chem.* **2016**, *88*, 3406–3412.
- (57) Sellies, L.; Reile, I.; Aspers, R. L. E. G.; Feiters, M. C.; Rutjes, F. P. J. T.; Tessari, M. Chem. Commun. 2019, 55, 7235–7238.
- (58) Ausmees, K.; Reimets, N.; Reile, I. Chem. Commun. 2022, 58, 463-466.
- (59) Trofimov, I. A.; Salnikov, O. G.; Chekmenev, E. Y.; Koptyug, I. V. Hyperpolarization of Spectator Molecules via PHIP-RASER. *The Parahydrogen Enhanced Resonance Meeting.* 2021, Day 2, p. 3, https://static1.squarespace.com/static/5ea725f5782b1b603bd2686f/t/60ccfab5beb0212573f9bd82/1624046261790/Day2+Abstracts+v2.pdf.

□ Recommended by ACS

Enhancing ¹⁹F Benchtop NMR Spectroscopy by Combining *para*-Hydrogen Hyperpolarization and Multiplet Refocusing

Ana I. Silva Terra, Meghan E. Halse, et al.

NOVEMBER 08, 2022

ACS MEASUREMENT SCIENCE AU

READ 🗹

Inversion of Hyperpolarized ¹³C NMR Signals through Cross-Correlated Cross-Relaxation in Dissolution DNP Experiments

Mattia Negroni, Dennis Kurzbach, et al.

JUNE 08, 2022

THE JOURNAL OF PHYSICAL CHEMISTRY B

READ 🗹

Enhanced Nuclear Magnetic Resonance Spectroscopy with Isotropic Mixing as a Pseudodimension

Dariusz Gołowicz, Krzysztof Kazimierczuk, et al.

JUNE 13, 2022

ANALYTICAL CHEMISTRY

RFAD **[**✓

Quantitation of Nuclear Magnetic Resonance Spectra at Earth's Magnetic Field

Derrick C. Kaseman, Robert F. Williams, et al.

NOVEMBER 08, 2021

ANALYTICAL CHEMISTRY

READ 🗹

Get More Suggestions >